European Radiology (2019) 29:6018–6028
https://doi.org/10.1007/s00330-019-06178-9

MOLECULAR IMAGING

Tumour necrosis as assessed with ^{18}F-FDG PET is a potential prognostic marker in diffuse large B cell lymphoma independent of *MYC* rearrangements

Xaver U. Kahle[1] · Menno Hovingh[1] · Walter Noordzij[2] · Annika Seitz[3] · Arjan Diepstra[3] · Lydia Visser[3] · Anke van den Berg[3] · Tom van Meerten[1] · Gerwin Huls[1] · Ronald Boellaard[2] · Thomas C. Kwee[4] · Marcel Nijland[1]

Received: 28 November 2018 / Revised: 28 February 2019 / Accepted: 18 March 2019 / Published online: 26 April 2019

Abstract

Objectives *MYC* gene rearrangements in diffuse large B cell lymphomas (DLBCLs) result in high proliferation rates and are associated with a poor prognosis. Strong proliferation is associated with high metabolic demand and tumour necrosis. The aim of this study was to investigate differences in the presence of necrosis and semiquantitative ^{18}F-FDG PET metrics between DLBCL cases with or without a *MYC* rearrangement. The prognostic impact of necrosis and semiquantitative ^{18}F-FDG PET parameters was investigated in an explorative survival analysis.

Methods Fluorescence in situ hybridisation analysis for *MYC* rearrangements, visual assesment, semiquantitative analysis of ^{18}F-FDG PET scans and patient survival analysis were performed in 61 DLBCL patients, treated at a single referral hospital between 2008 and 2015.

Results Of 61 tumours, 21 (34%) had a *MYC* rearrangement (*MYC*$^{+}$). *MYC* status was neither associated with the presence of necrosis on ^{18}F-FDG PET scans (necrosis^{PET}; $p = 1.0$) nor associated with the investigated semiquantitative parameters maximum standard uptake value (SUV_{max}; $p = 0.43$), single highest SUV_{max} ($p = 0.49$), metabolic active tumour volume (MATV; $p = 0.68$) or total lesion glycolysis (TLG; $p = 0.62$). A multivariate patient survival analysis of the entire cohort showed necrosis^{PET} as an independent prognostic marker for disease-specific survival (DSS) (HR = 13.9; 95% CI 3.0–65; $p = 0.001$).

Conclusions *MYC* rearrangements in DLBCL have no influence on the visual parameter necrosis^{PET} or the semi-quantiative parameters SUV_{max}, MATV and TLG. Irrespective of *MYC* rearrangements, necrosis^{PET} is an independent, adverse prognostic factor for DSS.

Key Points

- *Retrospective analysis indicates that MYC rearrangement is not associated with necrosis on ^{18}F-FDG PET (necrosis^{PET}) scans or semiquantitative ^{18}F-FDG PET parameters.*
- *Necrosis^{PET} is a potential independent adverse prognostic factor for disease-specific survival in patients with DLBCL and is not influenced by the presence of MYC rearrangements.*

Keywords Diffuse, large B cell, lymphoma · MYC oncogene · Necrosis · Fluorodeoxyglucose F18 · Positron emission tomography

Electronic supplementary material The online version of this article (https://doi.org/10.1007/s00330-019-06178-9) contains supplementary material, which is available to authorized users.

✉ Xaver U. Kahle
x.kahle@umcg.nl

[1] Department of Hematology, University of Groningen, University Medical Center Groningen, Groningen, The Netherlands

[2] Department of Nuclear Medicine and Molecular Imaging, University of Groningen, University Medical Center Groningen, Groningen, The Netherlands

[3] Department of Pathology and Medical Biology, University of Groningen, University Medical Center Groningen, Groningen, The Netherlands

[4] Department of Radiology, University of Groningen, University Medical Center Groningen, Groningen, The Netherlands

Abbreviations and acronyms

^{18}F-FDG	^{18}F-fluorodeoxyglucose
B-NHL	B cell non-Hodgkin lymphoma
CT	Computed tomography
DLBCL	Diffuse large B cell lymphoma
DSS	Disease-specific survival
FISH	Fluorescence in situ hybridisation
LDH	Lactate dehydrogenase
MATV	Metabolically active tumour volume (sum of all lesions within an individual patient)
NCCN-IPI	National Comprehensive Cancer Network international prognostic index
necrosis^{Hist}	Necrosis as assessed by histological scoring
necrosis^{PET}	Necrosis as assessed by ^{18}F-FDG PET
OS	Overall survival
PET	Positron emission tomography
PFS	Progression-free survival
SUV	Standard uptake value
SUV_{max}	Highest SUV per voxel within 1 lymphoma lesion (reported here as the mean of SUV_{max} of all lesions within an individual patient)
SUV_{max} single highest	Highest SUV_{max} of all lesions within an individual patient
TLG	Total lesion glycolysis (sum of all lesions within an individual patient)
WHO	World Health Organization.

Introduction

Diffuse large B cell lymphoma (DLBCL) accounts for 35% of all B cell non-Hodgkin lymphomas (B-NHL) [1]. Approximately 10–15% of DLBCL cases harbour a *MYC* gene rearrangement (*MYC*$^+$), as assessed by fluorescence in situ hybridisation (FISH) [2]. These lymphomas are characterised by a very high proliferation rate. Patients bearing a *MYC*$^+$ lymphoma experience an aggressive clinical course and have a poor prognosis when treated with the standard regimen of rituximab, cyclophosphamide, doxorubicin, vincristine and prednisolone (R-CHOP) [3]. In 2017, the World Health Organization (WHO) established a new entity for *MYC* rearranged DLBCL, called 'high-grade B-cell lymphoma with *MYC* and *BCL2* and/or *BCL6* rearrangements' [1, 4].

MYC is an oncogenic transcription factor regulating a vast array of cellular processes and pathways [5, 6]. Tumour cells overexpressing MYC meet their high energy demands by increased glucose uptake, glycolysis, lactate production and amino acid consumption [7, 8]. However, unlike physiological tissues, cancer cells frequently have acquired resistance to apoptosis and cannot regulate their energy expenditure during metabolic stress, resulting in cell death via necrosis when nutrient supply is compromised [9–11].

In B-NHL patients, ^{18}F-fluorodeoxyglucose positron emission tomography (^{18}F-FDG PET) scans are used for staging and response assessment [12]. Tumour necrosis can be assessed by visual inspection of ^{18}F-FDG PET scans (necrosis^{PET}) [13]. Necrosis can be observed in 14–20% of DLBCL cases and has been associated with an adverse prognosis [14, 15]. Semiquantitative assessment of ^{18}F-FDG PET allows for relative comparison of parameters based on the spatial distribution and degree of ^{18}F-FDG uptake, and is currently being investigated as a tool for therapy monitoring and assessing prognosis in B-NHL [16–18]. Still, data on the prognostic value of the semiquantitative parameters maximum standardised uptake value (SUV_{max}) and metabolically active tumour volume (MATV) in DLBCL are conflicting [19–21].

MYC rearrangement, tumour necrosis (necrosis^{PET}) and parameters derived from semiquantitative analysis of ^{18}F-FDG PET are fundamentally linked to metabolism, yet the relationship between these factors remains unknown. We hypothesise that the higher metabolic activity mediated by *MYC* rearrangements might result in a higher incidence of necrosis^{PET} and increased semiquantitative parameters. The previously suggested prognostic impact of necrosis^{PET} [15] and semiquantitative parameters [16–18] in DLBCL might be accredited to their potential association with *MYC* rearrangements.

Therefore, the aim of this study was to investigate differences in the presence of necrosis^{PET} and semiquantitative ^{18}F-FDG PET metrics between DLBCL cases with or without a *MYC* rearrangement. The prognostic impact of these factors was explored by means of survival analysis.

Materials and methods

Study design and case selection

For this retrospective single-centre study, consecutive patients with newly diagnosed, histologically confirmed DLBCL between 2008 and 2015 were identified in the electronic healthcare database of the University Medical Center Groningen (UMCG), a reference centre for aggressive B cell lymphomas. Cases of primary cutaneous DLBCL, primary central nervous system lymphoma, primary mediastinal B cell lymphoma and immunodeficiency-associated lymphomas were excluded. The selection of cases for this study is summarised in Fig. 1. Patients were stratified according to the National Comprehensive Cancer Network international prognostic index (NCCN-IPI) [22]. End of treatment response was assessed by ^{18}F-FDG PET/CT scan. Tumour responses were classified

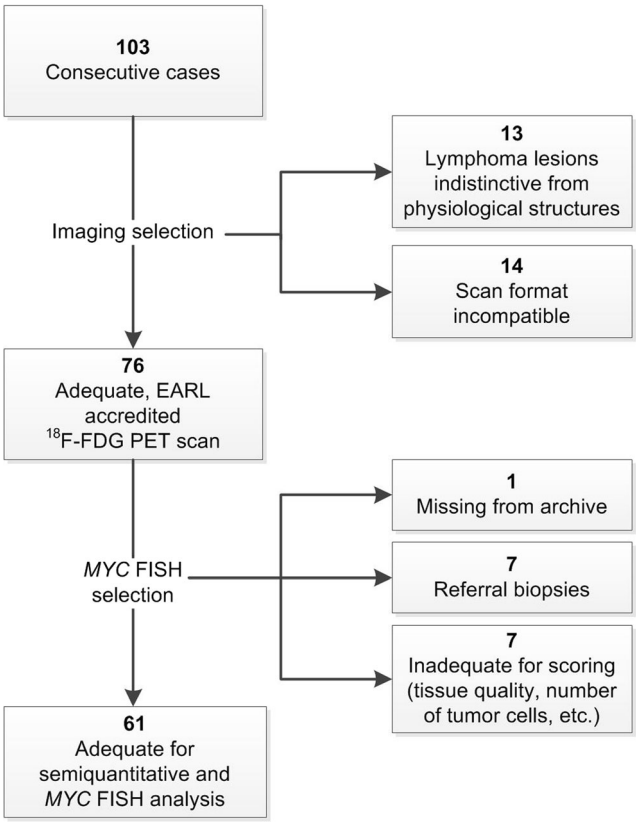

Fig. 1 Flow-chart of case selection

according to Lugano criteria [12]. Follow-up was registered until early October 2017. According to Dutch regulations, no medical ethical committee approval was required for this retrospective, non-interventional study. A waiver was obtained from the medical ethics committee of the UMCG on November 13, 2018. The study utilised rest material from patients, the use of which is regulated under the code for good clinical practice in the Netherlands and does not require informed consent in accordance with Dutch regulations.

Pathology review

Pathology review was done using the 2008 WHO classification of haematopoietic and lymphoid tissues (AD) [23]. Histological scoring for necrosis (necrosis^{Hist}) was done by microscopic assessment of haematoxylin and eosin–stained slides. Only microscopic areas with definite histopathological signs of necrosis (i.e. karyolysis) were scored as positive for necrosis^{Hist}.

MYC fluorescence in situ hybridisation

For evaluation of a *MYC* rearrangement, formalin-fixed paraffin-embedded tissue blocks of primary tumour samples were used. Interphase fluorescence in situ hybridisation (FISH) was performed on 4-μm-thick whole tissue sections, using Vysis break apart probes (Abbot Technologies) and standard FISH protocols as previously described [24]. Researchers performing *MYC* FISH analyses were blinded for results from visual scoring, microscopic assessment of necrosis (necrosis^{Hist}) and clinical outcome.

^{18}F-FDG PET imaging

All ^{18}F-FDG PET scans were performed prior to therapy. Patients were allowed to continue all medication and fasted for at least 6 h before whole-body (from the skull vertex to mid-thigh level) three-dimensional PET images were acquired. This was done 60 min after intravenous administration of a standard dose of 3 MBq/kg (0.081 mCi/kg) bodyweight ^{18}F-FDG on a Biograph mCT (Siemens Healthineers), according to the European Association of Nuclear Medicine (EANM) procedure guidelines for tumour imaging with FDG PET/CT (version 2.0) [25]. Acquisition was performed in seven bed positions of 2-min emission scans for patients 60–90 kg. Patients with body weight less than 60 kg and more than 90 kg body weight were scanned with 1 min and 3 min per bed position, respectively. Low-dose transmission CT was used for attenuation correction. Low-dose CT and ^{18}F-FDG PET scans were automatically fused by the use of three-dimensional fusion software (Siemens Healthineers) with manual fine adjustments. Raw data were reconstructed through ultra-high definition (Siemens Healthineers).

Computed tomography

Diagnostic CTs were acquired via integrated ^{18}F-FDG PET/CT scans according to the European Association of Nuclear Medicine (EANM) procedure guidelines for tumour imaging with FDG PET/CT (version 2.0) [25]. Bulky disease was defined as any nodal lymphoma lesion > 10 cm in coronal, axial or sagittal planes.

^{18}F-FDG PET analysis

All ^{18}F-FDG PET scans were visually assessed for the presence of tumour necrosis (necrosis^{PET}) by an experienced reader (TCK), who was blinded to clinical, laboratory, biopsy and follow-up findings, as previously described [15]. Areas within any nodal or extranodal ^{18}F-FDG PET–avid lymphomatous lesions that showed no ^{18}F-FDG uptake were registered as having necrosis^{PET} (Fig. 2); no specific visual scale was used. Semiquantitative analysis was performed using an in-house tool for quantitative ^{18}F-FDG PET/CT analysis, as previously described [26–28]. This programme automatically preselects lesions using a SUV_{max} threshold of 4 and a metabolic volume threshold of 2.5 ml. Unwanted preselected FDG-avid regions, such as the bladder and brain, are removed by user interaction. Finally, remaining FDG-avid segmentations are processed

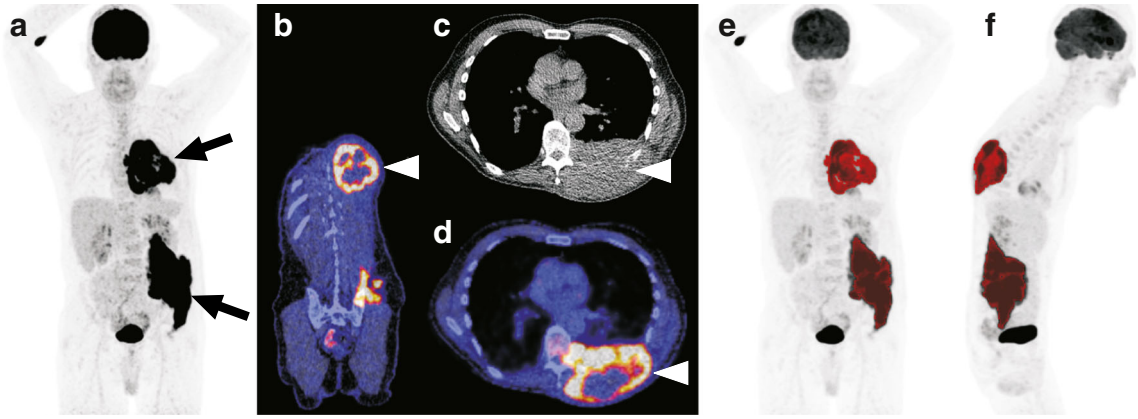

Fig. 2 Visual assessment of necrosis and semiquantitative ^{18}F-FDG PET review process. **a** A 65-year-old man with diffuse large B cell lymphoma (DLBCL) and tumour masses in the left dorsal chest wall and left pelvis, as shown on the coronal maximum intensity projection (MIP) ^{18}F-FDG PET image (arrows). Coronal fused ^{18}F-FDG PET/CT (**b**), axial CT (**c**) and axial fused ^{18}F-FDG PET/CT (**d**) show the tumour mass with photopenic areas (arrow heads), in keeping with tumour necrosis. Coronal and sagittal MIP ^{18}F-FDG PET images (**e** and **f**) show tumour segmentation (marked in red colour) for the calculation of metabolically active tumour volume (MATV), total lesion glycolysis (TLG), maximum standard uptake value (SUV_{max}), and single highest SUV_{max}

using a background-corrected 50% of SUV peak region growing method, as described by Frings et al [26], to obtain the final tumour segmentations. In case obvious lymphoma lesions were not selected ($n = 3$), they were manually added after automatic tumour segmentation. From the final segmentation, the metabolic active tumour volume (MATV, in ml),

Table 1 Demographics and baseline disease characteristics of patients with diffuse large B cell lymphoma according to *MYC* status

			MYC status				
	Total ($n = 61$)		*MYC*$^-$ ($n = 40$)		*MYC*$^+$ ($n = 21$)		*p* value
	No.	%	No.	%	No.	%	
Gender							
Male	36	59.0	24	60.0	12	57.1	1.0[a]
Female	25	41.0	16	40.0	9	42.9	
Age							
Median (range)	63 (26–91)		64 (26–91)		61 (30–79)		0.64[b]
Age ≤ 60 years	24	39.3	14	35.0	10	47.6	0.5[a]
Age > 60 years	37	60.7	26	65.0	11	52.4	
Stage							
I–II	22	36.0	15	37.5	7	33.3	0.97[a]
III–IV	39	63.9	25	62.5	14	66.7	
NCCN-IPI score							
0–3	30	49.2	22	55.0	8	38.1	0.32[a]
4–8	31	50.8	18	45.0	13	61.9	
Serum LDH							
Median (range)	282 (126–3037)		237 (126–1292)		381 (140–3037)		0.04[b]
Normal	29	47.5	22	55.0	7	33.3	0.18[a]
Elevated	32	52.5	18	45.0	14	66.7	
Treatment							
R-CHOP	56	91.8	37	92.5	19	90.5	0.36[c]
Intensive chemotherapy	3	4.9	1	2.5	2	9.5	
Palliative	2	3.3	2	5.0	0	0	

[a] Pearson's chi-square test with Yates' continuity correction

[b] Wilcoxon rank-sum test with continuity correction

[c] Fisher's exact test for count data

Table 2 Necrosis and semiquantitative ^{18}F-FDG PET parameters according to *MYC* status

	Total ($n = 61$)		*MYC* status				p value
			MYC^- ($n = 40$)		MYC^+ ($n = 21$)		
	No.	%	No.	%	No.	%	
$necrosis^{PET}$							
Absent	46	75.4	30	75.0	16	76.2	1.0[c]
Present	15	24.6	10	25.0	5	23.8	
$necrosis^{Hist}$							
Absent	42	68.9	28	70.0	14	66.7	0.52[c]
Present	16	26.2	11	27.5	5	23.8	
Not available	3	4.9	1	2.5	2	9.5	
SUV_{max}							
Median (range)	13.0 (3.0–38.4)		13.1 (3.0–33.9)		10.4 (5.8–38.4)		0.43[b]
SUV_{max} single highest							
Median (range)	18.8 (3.8–45.8)		19.7 (3.8–39.0)		14.2 (5.8–45.8)		0.49[b]
MATV							
Median (range)	154.7 (1–3774)		156.0 (1–2800)		154.7 (7–3774)		0.68[b]
TLG							
Median (range)	1387.4 (3–29,462)		1632.8 (3–29,462)		1147.1 (47–20,065)		0.62[b]

[b] Wilcoxon rank-sum test

[c] Fisher's exact test for count data

total lesion glycolysis (TLG = MATV × SUV_{mean}) and SUVs are derived for each lesion independently as well as summed over all lesions. Lesion selection and semiquantitative analysis was performed by MH under direct supervision of an experienced nuclear medicine physician (WN) and a nuclear physicist (RB). SUV_{max} was defined as the highest SUV per voxel within one lymphomatous lesion. In this paper, SUV_{max} is reported as the mean of SUV_{max} across all lesions of an individual patient. SUV_{max} single highest was defined as the highest SUV_{max} of all lesions within an individual patient.

Statistical analysis

Comparison between continuous, non-normally distributed variables was estimated by Wilcoxon rank-sum test. Differences between two nominal variables were evaluated using Pearson's chi-square or Fisher's exact test (for expected groups sizes ≤ 5). For exploratory survival analysis, the primary endpoints were overall survival (OS), progression-free survival (PFS) and disease-specific survival (DSS). OS was defined as the time from diagnosis until death (from any cause). PFS was defined as the time from diagnosis until death or relapse or progression [12]. DSS was defined as the time from diagnosis until death from DLBCL. Surviving patients were censored at the last date of follow-up. Survival curves were estimated according to the Kaplan-Meier method. Cox regression was used for univariate and multivariate survival analyses and results were reported as hazard ratio (HR), 95% confidence interval (CI) and p value based on statistical Wald test. A two-tailed p value of less than 0.05 indicated statistical significance. All analyses were performed using R version 3.4.1 and R-studio version 1.0.153 software.

Results

Patient characteristics

Characteristics of the entire cohort (61 patients) are summarised in Table 1. A total of 21 patients (34%) had a DLBCL harbouring a *MYC* rearrangement. *MYC* rearrangement was observed in 11 patients (21.6%) primarily seen in the UMCG ($n = 51$) and 10 patients (100%) referred from affiliated hospitals ($n = 10$). *MYC* groups did not differ with regard to baseline characteristics (Table 1) except for serum LDH levels, which were higher in the *MYC*-positive group ($p = 0.036$) than in cases without *MYC* rearrangement.

MYC status, necrosis and semiquantitative ^{18}F-FDG PET parameters

$necrosis^{PET}$ was observed in 15 patients (25%). The relationships between *MYC* status and $necrosis^{PET}$, $necrosis^{Hist}$ and semiquantitative ^{18}F-FDG PET parameters are summarised in Table 2. MYC^+ cases did not differ from cases without

Table 3 Univariate analysis of patient characteristics and semiquantitative ^{18}F-FDG PET parameters on overall survival, progression-free survival and disease-specific survival

	Hazard ratio OS	95% CI	*p* value (Wald test)	Hazard ratio PFS	95% CI	*p* value (Wald test)	Hazard ratio DSS	95% CI	*p* value (Wald test)
MYC									
MYC-negative	Reference			Reference			Reference		
MYC-positive	2.9	1.1–7.4	0.025*	2.3	0.97–5.7	0.058	6.3	1.7–24	0.007**
NCCN-IPI									
0–3	Reference			Reference			Reference		
4–8	3.0	1.0–8.3	0.04*	3.6	1.3–10	0.013*	10.7	1.4–84	0.024*
necrosis^{PET}									
Absent	Reference			Reference			Reference		
Present	1.7	0.6–4.5	0.3	1.8	0.7–4.6	0.2	3.9	1.2–13	0.025*
SUV_{max}									
< Median	Reference			Reference			Reference		
≥ Median	0.4	0.1–1.1	0.08	0.4	0.2–1.1	0.08	0.2	0.05–1.1	0.06
SUV_{max} single highest									
< Median	Reference			Reference			Reference		
≥ Median	0.3	0.09–0.9	0.026*	0.4	0.2–1.1	0.07	0.1	0.01–0.8	0.028*
MATV									
< Median	Reference			Reference			Reference		
≥ Median	1.1	0.4–2.7	0.9	1.3	0.5–3.1	0.59	2.8	0.7–10.6	0.14
Single lesion MATV†									
< Median	Reference			Reference			Reference		
≥ Median	1.2	0.5–3.2	0.69	1.5	0.6–3.7	0.39	2.5	0.6–9.6	0.19
TLG									
< Median	Reference			Reference			Reference		
≥ Median	0.6	0.2–1.6	0.31	0.8	0.3–1.9	0.57	1.1	0.3–3.8	0.84

† Volume of the single largest/necrotic lesion; * = significance level of $p < 0.05$; ** = significance level of $p < 0.01$

MYC rearrangement with regard to necrosis^{PET} ($p = 1.0$) or necrosis^{Hist} ($p = 0.52$).

When the semiquantitative parameters SUV_{max}, SUV_{max} single highest, MATV and TLG were studied, no difference between *MYC* groups was observed. There was no relation between the presence of necrosis^{PET} and necrosis^{Hist} ($p = 0.1$; Supplementary Figure 1).

Necrosis^{PET} and tumour volume

In 14 of 15 necrosis^{PET} cases, necrosis was observed in the largest lesion. In comparison, the largest individual lesion of cases without necrosis^{PET} had a significantly lower MATV ($p = 0.0006$) and SUV_{max} ($p = 0.02$), irrespective of *MYC* status (Supplementary Figure 2). Bulky disease was observed in 24 patients (39%). Bulky disease was significantly correlated with necrosis^{PET} ($p = 0.005$), but not with *MYC* status ($p = 0.9$) or necrosis^{Hist} ($p = 0.8$). Extranodal growth of lesions was not significantly correlated with the presence of necrosis^{PET} ($p = 0.26$).

Survival analysis

The median follow-up was 34 months. At 5 years, OS was 67% (95% CI 54–83%), PFS was 65% (95% CI 53–81%) and DSS was 81% (95% CI 70–93%) for the entire cohort. Of the seven deaths unrelated to lymphoma, two were caused by metastatic adenocarcinoma, two were due to cardiac failure, one was due to acute on chronic renal failure and there were two cases of sudden deaths in patients in complete remission of DLBCL.

Results of the univariate Cox regression analysis (HR, 95% CI and *p* value) are shown in Table 3. The univariate analysis for OS identified *MYC*, NCCN-IPI and SUV_{max} single highest as associated factors. In univariate analysis for PFS, only NCCN-IPI was associated with outcome. In the univariate analysis for DSS *MYC*, NCCN-IPI, SUV_{max} single highest and necrosis^{PET} were associated. Both SUV_{max} and SUV_{max} single highest showed negative beta-coefficients throughout the univariate survival analysis.

For multivariate analysis, the parameters *MYC*, NCCN-IPI, necrosis^{PET} and SUV_{max} single highest were used due to their

Table 4 Multivariate analysis of patient characteristics on overall survival, progression-free survival and disease-specific survival

	Hazard ratio OS	95% CI	*p* value (Wald test)	*p* value model (Wald test)
MYC				0.004
MYC-negative	Reference			
MYC-positive	3.1	1.1–8.7	0.029*	
NCCN-IPI				
0–3	Reference			
4–8	2.4	0.8–6.9	0.116	
necrosis^{PET}				
Absent	Reference			
Present	2.6	0.9–7.7	0.079	
SUV_{max} single highest				
< Median	Reference			
≥ Median	0.3	0.1–0.9	0.027*	
	Hazard ratio PFS	95% CI	*p* value (Wald test)	*p* value model (Wald test)
MYC				0.005
MYC-negative	Reference			
MYC-positive	2.4	0.9–6.3	0.07	
NCCN-IPI				
0–3	Reference			
4–8	3.2	1.1–9.0	0.028*	
necrosis^{PET}				
Absent	Reference			
Present	2.6	1.0–7.0	0.06	
SUV_{max} single highest				
< Median	Reference			
≥ Median	0.4	0.2–1.1	0.08	
	Hazard ratio DSS	95% CI	*p* value (Wald test)	*p* value model (Wald test)
MYC				0.0007
MYC-negative	Reference			
MYC-positive	14.6	2.6–82	0.002**	
NCCN-IPI				
0–3	Reference			
4–8	6.5	0.6–66	0.113	
necrosis^{PET}				
Absent	Reference			
Present	13.3	2.8–63	0.001**	
SUV_{max} single highest				
< Median	Reference			
≥ Median	0.12	0.01–1.2	0.075	

* = significance level of $p < 0.05$; ** = significance level of $p < 0.01$

prognostic impact on lymphoma-related deaths in univariate analysis (Table 4). Necrosis^{PET} did not contribute to the prognostic model for OS and PFS. However, for DSS, necrosis^{PET} had a large adverse prognostic impact and proved to be independent (HR = 13.9; 95% CI 3.0–65; $p = 0.001$). The Kaplan-Meier analysis for DSS showed no events during the 5-year follow-up period for patients who neither had *MYC* rearrangements nor had necrosis^{PET} ($n = 30$) (Fig. 3).

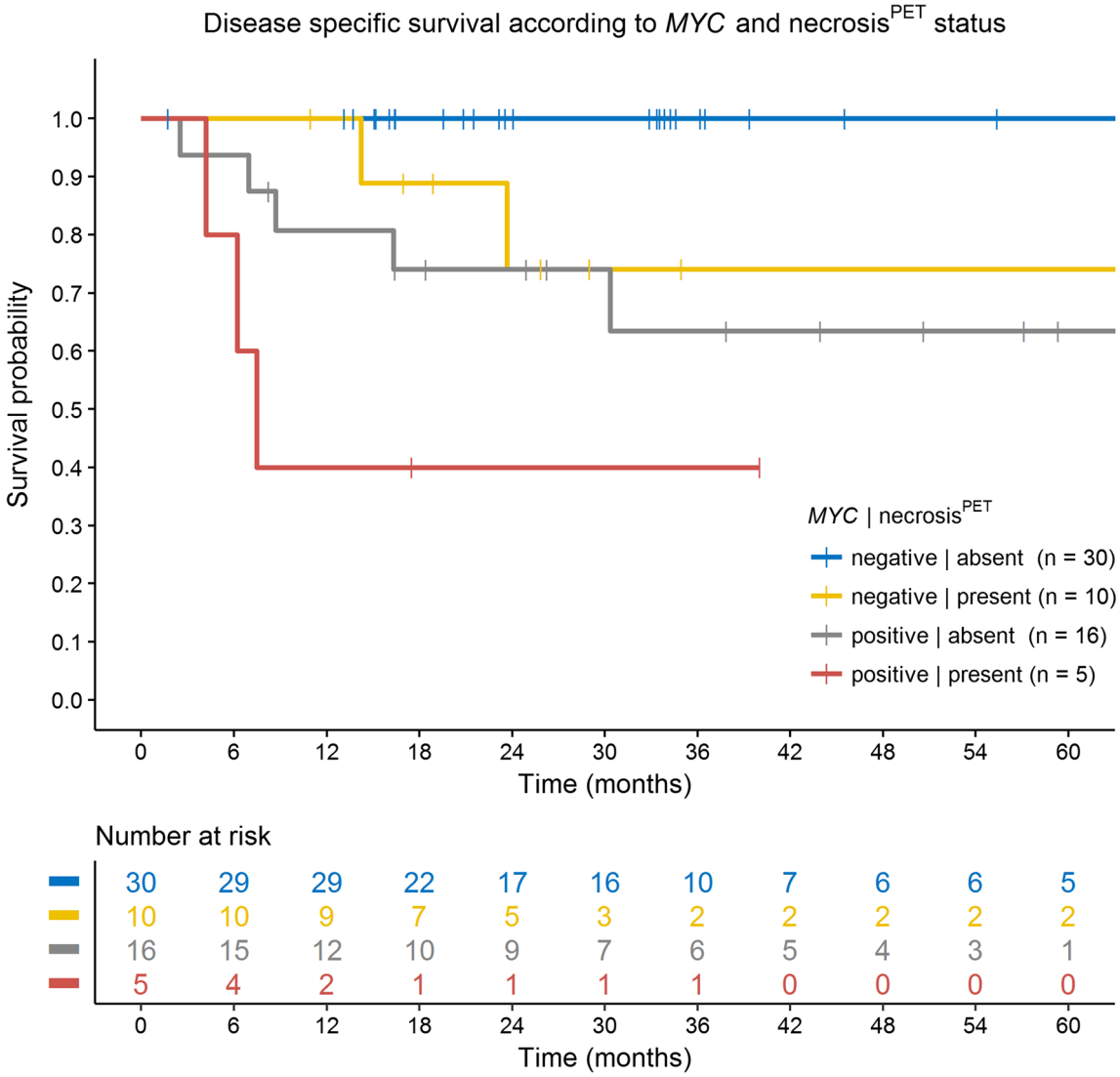

Fig. 3 Kaplan-Meier curve showing disease-specific survival according to combined analysis with *MYC* rearrangement status and necrosis^{PET} (log-rank test, $p = 0.00022$). No events were observed in patients without *MYC* rearrangement and who had no necrosis^{PET}

Discussion

Based on the current investigation, there is no association of *MYC* rearrangements with the presence of tumour necrosis assessed by ^{18}F-FDG PET or the semiquantitative ^{18}F-FDG PET parameters SUV_{max}, SUV_{max} single highest, MATV and TLG. We therefore rejected the hypothesis that metabolic changes induced by *MYC* rearrangements might increase the incidence of necrosis^{PET} or alter the profile of semiquantitative parameters in DLBCL. Necrosis^{PET} was significantly associated with the MATV of the single largest tumour lesion. The SUV_{max} of the single largest necrosis^{PET} lesion was significantly higher compared with the lesions without necrosis^{PET}. Both of these observations support the notion of larger, more metabolically active tumours being more susceptible to necrosis, irrespective of *MYC* status.

Our analyses demonstrate that necrosis^{PET} had a significant impact on DSS, thereby substantiating previous findings about the prognostic value of this visual marker [15]. The presented data show that the presence of *MYC* rearrangement, in itself a powerful predictive factor, is not related to necrosis^{PET}. This allows for integration of *MYC* status and necrosis^{PET} into a prognostic model for DLBCL. When combined with *MYC*, NCCN-IPI and SUV_{max} single highest in the multivariate analysis, necrosis^{PET} had the highest significance in predicting death due to lymphoma and a higher prognostic impact than NCCN-IPI, the currently most accurate prognostic index for DLBCL [22]. Thus, our results support the potential additive value of necrosis^{PET} as an important biomarker for risk stratification in the clinical setting [14, 15].

The lack of a relationship between *MYC* rearrangements and semiquantitative ^{18}F-FDG PET metrics might have several causes. First, proliferation in DLBCL could be independent of *MYC* rearrangement. This would only partially explain the lack of relationship, since the median proliferation index

(Ki-67 staining) of MYC^+ DLBCL is universally high (> 90%) in contrast to the much broader range observed in MYC^- DLBCL [29]. Second, overexpression of MYC via other mechanisms such as epigenetic pathways might explain increased glucose uptake in *MYC* FISH–negative DLBCL. This is supported by studies showing high MYC protein expression in 19–40% of DLBCL cases [30–32]. Cottereau et al previously reported a lack of relation between MYC protein expression and ^{18}F-FDG PET parameters in DLBCL [19]. However, FISH analysis, which is considered the gold standard examination for *MYC* rearrangements [33–35], was not performed. Third, high metabolic activity might be induced by alternative changes in metabolic drivers, such as mutations in PTEN (observed in approximately 15% of DLBCL) that lead to activation of the P13K/AKT/mTOR pathway [29, 36–38].

Intriguingly, the univariate survival analysis indicated a protective effect for cases with SUV_{max} and SUV_{max} single highest measurements above the median. Studies on the prognostic impact of these variables are conflicting [20, 39–41]. Gallicchio et al published results similar to ours, alluding to lymphomas with high metabolic activity being more responsive to chemotherapy [20]. In light of conflicting data on the prognostic value of semiquantitative ^{18}F-FDG PET parameters [19–21, 42, 43], our results underline the need for larger, prospective studies with external validation cohorts [42].

This study has several limitations. First there is a referral bias with a high incidence of MYC^+ cases (34%) in our dataset. The enrichment in our study can largely be explained by the fact that, as a reference centre, aggressive and MYC^+ DLBCL cases (including suspected cases of Burkitt lymphoma which subsequently prove to be MYC^+ DLBCL) are referred to our site. Second, the total number of cases with necrosis^{PET} is small, which increases the risk of a sampling error. Nevertheless, the incidence of necrosis^{PET} in our study is in line with previous studies [13–15]. Furthermore, patients were included irrespective of their comorbidities. Factors like differences in treatment regimen and non-cancer-related deaths might thus have a large impact on the statistical analysis. This is supported by the difference between DSS and OS. Despite its limitations, the prognostic potential of *MYC* status and NCCN-IPI was reproduced in this dataset, making it a representative set of DLBCL cases. Larger prospective studies are warranted to validate the prognostic value of necrosis^{PET}.

Conclusion

In this comprehensive analysis of *MYC* rearranged DLBCL, we showed that a fundamental pathological change such as *MYC* rearrangement, which by itself has a significant impact on prognosis, has no influence on the presence of necrosis^{PET} or semiquantitative ^{18}F-FDG PET metrics. An explorative survival analysis suggests that the presence of necrosis determined by visual assessment of ^{18}F-FDG PET scans is an independent predictor of disease-specific survival in patients with DLBCL, regardless of *MYC* status.

Funding The authors state that this work has not received any funding.

Compliance with ethical standards

Guarantor The scientific guarantor of this publication is M. Nijland.

Conflict of interest The authors declare no relationships with any companies, whose products or services may be related to the subject matter of the article.

Statistics and biometry No complex statistical methods were necessary for this paper.

Informed consent Written informed consent was not required for this study. This study utilised rest material from patients, the use of which is regulated under the code for good clinical practice in the Netherlands and does not require informed consent in accordance with Dutch regulations.

Ethical approval According to Dutch regulations, no medical ethical committee approval was required for this retrospective, observational study. A waiver was obtained from the medical ethics committee of the UMCG on November 13, 2018.

Methodology This is a retrospective observational study performed at one institution.

References

1. International Agency for Research on Cancer (2017) WHO classification of tumours of haematopoietic and lymphoid tissues. Revised 4th edition 2017. WHO, Lyon
2. Aukema SM, Siebert R, Schuuring E et al (2011) Double-hit B-cell lymphomas. Blood 117:2319–2331. https://doi.org/10.1182/blood
3. Barrans S, Crouch S, Smith A et al (2010) Rearrangement of MYC is associated with poor prognosis in patients with diffuse large B-cell lymphoma treated in the era of rituximab. J Clin Oncol 28: 3360–3365. https://doi.org/10.1200/JCO.2009.26.3947
4. Jiang M, Bennani NN, Feldman AL (2017) Lymphoma classification update: B-cell non-Hodgkin lymphomas. Expert Rev Hematol 10:405–415. https://doi.org/10.1080/17474086.2017.1318053
5. Zeller KI, Jegga AG, Aronow BJ et al (2003) An integrated database of genes responsive to the Myc oncogenic transcription factor: identification of direct genomic targets. Genome Biol 4:R69. https://doi.org/10.1186/gb-2003-4-10-r69
6. DeBerardinis RJ, Lum JJ, Hatzivassiliou G, Thompson CB (2008) The biology of cancer: metabolic reprogramming fuels cell growth and proliferation. Cell Metab 7:11–20. https://doi.org/10.1016/j.cmet.2007.10.002

7. Miller DM, Thomas SD, Islam A et al (2012) c-Myc and cancer metabolism. Clin Cancer Res 18:5546–5553. https://doi.org/10.1158/1078-0432.CCR-12-0977
8. Dang CV, Le A, Gao P (2009) MYC-induced cancer cell energy metabolism and therapeutic opportunities. Clin Cancer Res 15:6479–6483. https://doi.org/10.1158/1078-0432.CCR-09-0889
9. Jin S, DiPaola RS, Mathew R, White E (2007) Metabolic catastrophe as a means to cancer cell death. J Cell Sci 120:379–383. https://doi.org/10.1242/jcs.03349
10. Jin S, White E (2007) Role of autophagy in cancer: management of metabolic stress. Autophagy 3:28–31
11. Proskuryakov SY, Gabai VL (2010) Mechanism of tumor cell necrosis. Curr Pharm Des 16:56–68
12. Cheson BD, Fisher RI, Barrington SF et al (2014) Recommendations for initial evaluation, staging, and response assessment of hodgkin and non-hodgkin lymphoma: the Lugano classification. J Clin Oncol 32:3059–3068. https://doi.org/10.1200/JCO.2013.54.8800
13. Song MK, Chung JS, Shin DY et al (2017) Tumor necrosis could reflect advanced disease status in patients with diffuse large B cell lymphoma treated with R-CHOP therapy. Ann Hematol 96:17–23. https://doi.org/10.1007/s00277-016-2822-8
14. Adams HJA, de Klerk JMH, Fijnheer R et al (2015) Prognostic value of tumor necrosis at CT in diffuse large B-cell lymphoma. Eur J Radiol 84:372–377. https://doi.org/10.1016/j.ejrad.2014.12.009
15. Adams HJA, de Klerk JMH, Fijnheer R et al (2016) Tumor necrosis at FDG-PET is an independent predictor of outcome in diffuse large B-cell lymphoma. Eur J Radiol 85:304–309. https://doi.org/10.1016/j.ejrad.2015.09.016
16. Barrington SF, Kluge R (2017) FDG PET for therapy monitoring in Hodgkin and non-Hodgkin lymphomas. Eur J Nucl Med Mol Imaging 44:97–110. https://doi.org/10.1007/s00259-017-3690-8
17. Xie M, Wu K, Liu Y et al (2015) Predictive value of F-18 FDG PET/CT quantization parameters in diffuse large B cell lymphoma: a meta-analysis with 702 participants. Med Oncol 32:446. https://doi.org/10.1007/s12032-014-0446-1
18. Dührsen U, Müller S, Hertenstein B et al (2018) Positron emission tomography-guided therapy of aggressive non-Hodgkin lymphomas (PETAL): a multicenter, randomized phase III trial. J Clin Oncol 36:2024–2034. https://doi.org/10.1200/JCO
19. Cottereau A-S, Lanic H, Mareschal S et al (2016) Molecular profile and FDG-PET/CT total metabolic tumor volume improve risk classification at diagnosis for patients with diffuse large B-cell lymphoma. Clin Cancer Res 22:3801–3809. https://doi.org/10.1158/1078-0432.CCR-15-2825
20. Gallicchio R, Mansueto G, Simeon V et al (2014) F-18 FDG PET/CT quantization parameters as predictors of outcome in patients with diffuse large B-cell lymphoma. Eur J Haematol 92:382–389. https://doi.org/10.1111/ejh.12268
21. Adams HJA, de Klerk JMH, Fijnheer R et al (2015) Prognostic superiority of the National Comprehensive Cancer Network International Prognostic Index over pretreatment whole-body volumetric-metabolic FDG-PET/CT metrics in diffuse large B-cell lymphoma. Eur J Haematol 94:532–539. https://doi.org/10.1111/ejh.12467
22. Zhou Z, Sehn LH, Rademaker AW et al (2014) An enhanced International Prognostic Index (NCCN-IPI) for patients with diffuse large B-cell lymphoma treated in the rituximab era. Blood 123:837–842. https://doi.org/10.1182/blood
23. International Agency for Research on Cancer (2008) WHO classification of tumours of haematopoeitic and lymphoid tissues. 4th edition 2008 WHO, Lyon
24. van der Wekken AJ, Pelgrim R, 't Hart N et al (2017) Dichotomous ALK-IHC is a better predictor for ALK inhibition outcome than traditional ALK-FISH in advanced non-small cell lung cancer. Clin Cancer Res 23:4251–4258. https://doi.org/10.1158/1078-0432.CCR-16-1631
25. Boellaard R, Delgado-Bolton R, Oyen WJG et al (2015) FDG PET/CT: EANM procedure guidelines for tumour imaging: version 2.0. Eur J Nucl Med Mol Imaging 42:328–354. https://doi.org/10.1007/s00259-014-2961-x
26. Frings V, van Velden FHP, Velasquez LM et al (2014) Repeatability of metabolically active tumor volume measurements with FDG PET/CT in advanced gastrointestinal malignancies: a multicenter study. Radiology 273:539–548. https://doi.org/10.1148/radiol.14132807
27. Cheebsumon P, van Velden FH, Yaqub M et al (2011) Measurement of metabolic tumor volume: static versus dynamic FDG scans. EJNMMI Res 1:35. https://doi.org/10.1186/2191-219X-1-35
28. Cheebsumon P, Boellaard R, de Ruysscher D et al (2012) Assessment of tumour size in PET/CT lung cancer studies: PET- and CT-based methods compared to pathology. EJNMMI Res 2:56. https://doi.org/10.1186/2191-219X-2-56
29. Agarwal R, Lade S, Liew D et al (2016) Role of immunohistochemistry in the era of genetic testing in *MYC*-positive aggressive B-cell lymphomas: a study of 209 cases. J Clin Pathol 69:266–270. https://doi.org/10.1136/jclinpath-2015-203002
30. Johnson NA, Slack GW, Savage KJ et al (2012) Concurrent expression of MYC and BCL2 in diffuse large B-cell lymphoma treated with rituximab plus cyclophosphamide, doxorubicin, vincristine, and prednisone. J Clin Oncol 30:3452–3459. https://doi.org/10.1200/JCO.2011.41.0985
31. Horn H, Ziepert M, Becher C et al (2013) MYC status in concert with BCL2 and BCL6 expression predicts outcome in diffuse large B-cell lymphoma. Blood 121:2253–2263. https://doi.org/10.1182/blood-2012-06
32. Valera A, López-Guillermo A, Cardesa-Salzmann T et al (2013) MYC protein expression and genetic alterations have prognostic impact in patients with diffuse large B-cell lymphoma treated with immunochemotherapy. Haematologica 98:1554–1562. https://doi.org/10.3324/haematol.2013.086173
33. Tilly H, Gomes Da Silva M, Vitolo U et al (2015) Diffuse large B-cell lymphoma (DLBCL): ESMO Clinical Practice Guidelines for diagnosis, treatment and follow-up. Ann Oncol 26(Suppl. 5):116–125. https://doi.org/10.1093/annonc/mdv304
34. Nguyen L, Papenhausen P, Shao H (2017) The role of c-MYC in B-cell lymphomas: diagnostic and molecular aspects. Genes (Basel) 8:E116. https://doi.org/10.3390/genes8040116
35. Sesques P, Johnson NA (2017) Approach to the diagnosis and treatment of high-grade B-cell lymphomas with MYC and BCL2 and/or BCL6 rearrangements. Blood 129:280–288. https://doi.org/10.1182/blood-2016-02
36. Tsukamoto N, Kojima M, Hasegawa M et al (2007) The usefulness of ^{18}F-fluorodeoxyglucose positron emission tomography (^{18}F-FDG-PET) and a comparison of ^{18}F-FDG-PET with ^{67}gallium scintigraphy in the evaluation of lymphoma: relation to histologic subtypes based on the World Health Organization classification. Cancer 110:652–659. https://doi.org/10.1002/cncr.22807
37. Frick M, Dörken B, Lenz G (2011) The molecular biology of diffuse large B-cell lymphoma. Ther Adv Hematol 2:369–379. https://doi.org/10.1177/2040620711419001
38. Barrington SF, Mikhaeel NG, Kostakoglu L et al (2014) Role of imaging in the staging and response assessment of lymphoma: consensus of the International Conference on Malignant Lymphomas Imaging Working Group. J Clin Oncol 32:3048–3058. https://doi.org/10.1200/JCO.2013.53.5229
39. Chihara D, Oki Y, Onoda H et al (2011) High maximum standard uptake value (SUVmax) on PET scan is associated with shorter survival in patients with diffuse large B cell lymphoma. Int J Hematol 93:502–508. https://doi.org/10.1007/s12185-011-0822-y
40. Park S, Moon SH, Park LC et al (2012) The impact of baseline and interim PET/CT parameters on clinical outcome in patients with

diffuse large B cell lymphoma. Am J Hematol 87:937–940. https://doi.org/10.1002/ajh.23267

41. Miyazaki Y, Nawa Y, Miyagawa M et al (2013) Maximum standard uptake value of ^{18}F-fluorodeoxyglucose positron emission tomography is a prognostic factor for progression-free survival of newly diagnosed patients with diffuse large B cell lymphoma. Ann Hematol 92:239–244. https://doi.org/10.1007/s00277-012-1602-3
42. Schröder H, Moskowitz C (2016) Metabolic tumor volume in lymphoma: hype or hope? J Clin Oncol 34:3591–3594
43. Schöder H, Zelenetz AD, Hamlin P et al (2016) Prospective study of 3'-deoxy-3'-^{18}F-fluorothymidine PET for early interim response assessment in advanced-stage B-cell lymphoma. J Nucl Med 57:728–734. https://doi.org/10.2967/jnumed.115.166769